Table S1. 38 stress-related vegetation indices in the literature used in the study for SVM modeling.

No.	Name	Formula	Reference*
1	Carter	R_{695}/R_{420}	[1]
2	Carter2	R_{695}/R_{760}	[1]
3	Carter3	R_{605}/R_{760}	[1]
4	Carter4	R_{710}/R_{760}	[1]
5	Carter5	R_{695}/R_{670}	[1]
6	Carter6	R_{550}	[1]
7	CI	$R_{675}*R_{690}/R^2_{683}$	[2]
8	D730/D706	D_{730}/D_{706}	[2]
9	DDI	$(R_{720+\Delta} - R_{720}) - (R_{672+\Delta} - R_{672})$	[3]
10	DPI	$(D_{688} * D_{710})/D^2_{697}$	[2]
11	DWSI2	R_{800}/R_{1660}	[4]
12	DWSI	R_{1660}/R_{550}	[4]
13	DWSI3	R_{1660}/R_{680}	[4]
14	DWSI4	R_{550}/R_{680}	[4]
15	DWSI5	$(R_{800} + R_{550})/(R_{1660} + R_{680})$	[4]
16	EGFN	$\frac{(max(D_{650:750}) - max(D_{500:550}))}{(max(D_{650:750}) + max(D_{500:550}))}$	[5]
17	EGFR	$max(D_{650:750})/max(D_{500:550})$	[5]
18	MPRI	$(R_{515} - R_{530})/(R_{515} + R_{530})$	[6]
19	MCARI	$((R_{700} - R_{670}) - 0.2 * (R_{700} - R_{550})) * (R_{700}/R_{670})$	[7]
20	MSI	R_{1600}/R_{817}	[8]
21	MTCI	$(R_{754} - R_{709})/(R_{709} - R_{681})$	[9]
22	NDVI	$(R_{800} - R_{680})/(R_{800} + R_{680})$	[10]
23	NPCI	$(R_{680} - R_{430})/(R_{680} + R_{430})$	[5]
24	PRI	$(R_{531} - R_{570})/(R_{531} + R_{570})$	[11]
25	PRI_norm	$PRI * (-1)/(RDVI * R_{700}/R_{670})$	[12]
26	PRI*CI2	PRI*CI2	[13]
27	PSSR	R_{800}/R_{635}	[14]
28	PSND	$(R_{800} - R_{470})/(R_{800} + R_{470})$	[14]
29	REP_LE	Red-edge position through linear extrapolation	[15]
30	SR7	R_{440}/R_{690}	[16]
31	SR8	R_{515}/R_{550}	[17]
32	SRWI	R_{850}/R_{1240}	[2]
33	Sum_Dr1	$\sum_{i=626}^{795} D1_i$	[18]
34	Sum_Dr2	$\sum_{i=680}^{780} D1_i$	[19]
35	Vogelmann	R_{740}/R_{720}	[20]
36	Vogelmann2	$(R_{734} - R_{747})/(R_{715} + R_{726})$	[20]
37	D715/705	D_{715}/D_{705}	[20]
38	Vogelmann4	$(R_{734} - R_{747})/(R_{715} + R_{720})$	[20]

Table S2. Detailed information on leaf samples.

Leaf Samples No.	Cultivar	Plant ID Per Cultivar	Type
1	8H534	2	healthy
2	8H534	3	healthy
3	DH351	1	healthy
4	DH351	3	healthy
5	Chang7-2	2	healthy

6	Chang7-2	3	healthy
7	8H953	5	healthy
8	8H953	6	healthy
9	PH6WC	7	healthy
10	PH6WC	8	healthy
11	DH351	5	healthy
12	DH351	6	healthy
13	Jing92	4	healthy
14	Jing92	8	healthy
15	Jing92	9	healthy
16	Jing724	5	healthy
17	Jing724	7	healthy
18	Jing724	8	healthy
19	8H534	6	Light
20	8H534	7	Light
21	DH351	7	Light
22	DH351	6	Light
23	Jing724	7	Light
24	Jing724	6	Light
25	Jing92	2	Light
26	Jing92	3	Light
27	DH382	3	Light
28	DH382	4	Light
29	Jing92	5	Light
30	Jing92	4	Light
31	Chang7-2	7	Light
32	Chang7-2	8	Light
33	PH6WC	4	Light
34	PH6WC	5	Light
35	8H534	8	Medium
36	8H953	9	Medium
37	Jing92	1	Medium
38	Jing92	4	Medium
39	Jing724	5	Medium
40	PH6WC	9	Medium
41	DH351	5	Medium
42	DH382	4	Medium
43	DH382	9	Medium
44	Chang7-2	7	Medium
45	Chang7-2	6	Medium
46	8H534	5	Severe
47	DH382	1	Severe
48	DH351	10	Severe
49	8H953	10	Severe
50	Chang7-2	6	Severe
51	Chang7-2	10	Severe
52	Jing724	3	Severe
53	Jing92	4	Severe
54	PH6WC	10	Severe

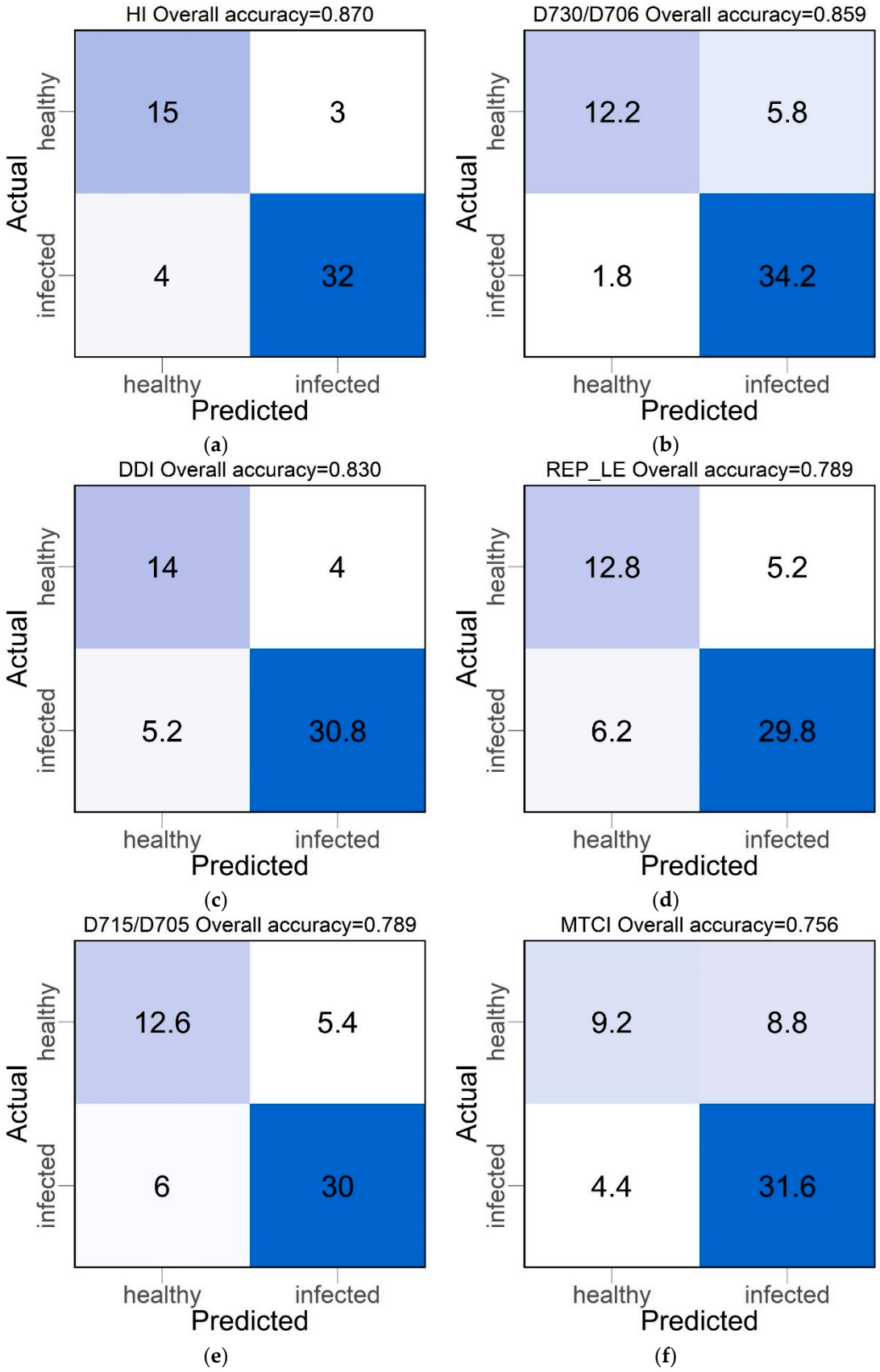

Figure S1. Averaged confusion matrix of different SCR detection models using support vector machine based 10-fold cross validation: a. Health Index (HI); b. The ratio of first derivative values at 730-706nm (D730/D706); c. Double Difference Index (DDI); d. The Red-edge position through linear extrapolation (REP_LE); e. The ratio of first derivative values at 715-705nm (D715/D705); f. MERIS

Terrestrial Chlorophyll Index (MTCI); the fraction number in the matrix was from the 10-fold cross validation results divided by ten.

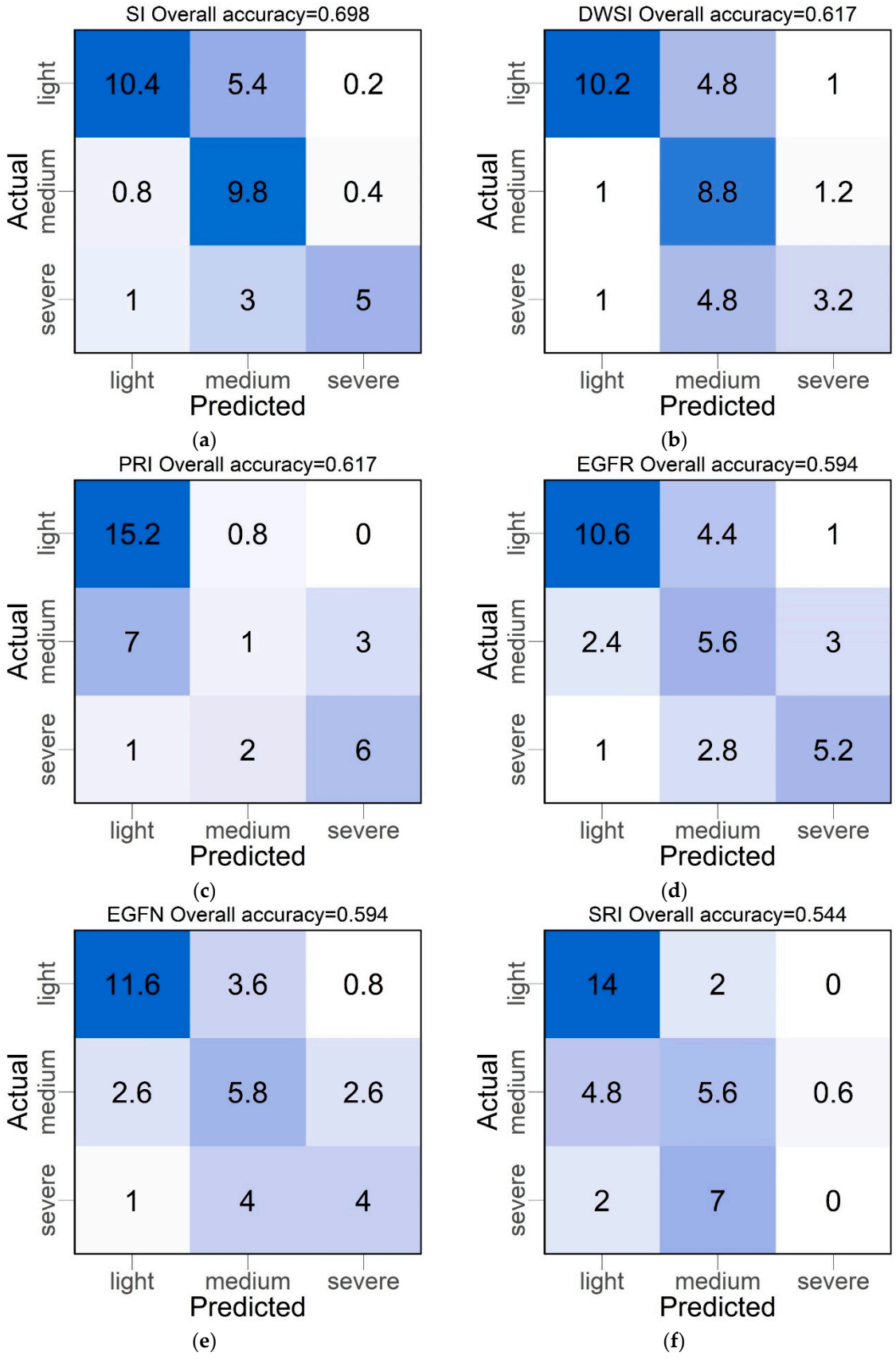

Figure S2. Averaged confusion matrix of different SCR severity models using support vector machine based 10-fold cross validation: a. Severity Index (SI); b. Disease-Water Stress Index (DWSI); c.

Physiological Reflectance Index (PRI); d. The simple ratio between the maxima of the first derivatives of reflectance at the red edge and green regions (EGFR); e. The normalized ratio between the maxima of the first derivatives of reflectance at the red edge and green regions (EGFN); f. Simple Ratio Index (SRI); the fraction number in the matrix was from the 10-fold cross validation results divided by ten.

Reference

1. Carter, G. A. Ratios of leaf reflectance in narrow wavebands as indicators of plant stress. *Int J Remote Sens.* **1994**, *15*, 697–703.
2. Zarco-Tejada, P. J.; Pushnik, J. C.; Dobrowski, S.; Ustin, S. L. Steady-state chlorophyll a fluorescence detection from canopy derivative reflectance and double-peak red-edge effects. *Remote Sens. Environ.* **2013,** *84*, 283–294.
3. le Maire, G.; Francois, C.; Dufrene, E. Towards universal broad leaf chlorophyll indices using PROSPECT simulated database and hyperspectral reflectance measurements. *Remote Sens. Environ.* **2004,** *89*, 1–28.
4. Apan, A.; Held, A.; Phinn, S.; Markley, J.; Jan. Detecting sugarcane "orange rust" disease using EO-1 Hyperion hyperspectral imagery. *Int J Remote Sens.* **2004,** *25*, 489–498.
5. Peñuelas, J.; Gamon, J. A.; Fredeen, A. L.; Merino, J.; Field, C. B. Reflectance indexes associated with physiological-changes in nitrogen-limited and water-limited sunflower leaves. *Remote Sens. Environ.* **1994,** *48*, 135–146.
6. Hernández-Clemente, R.; Navarro-Cerrillo, R. M.; Suárez, L.; Morales, F.; Zarco-Tejada, P. J. Assessing structural effects on PRI for stress detection in conifer forests. *Remote Sens. Environ.* **2011,** *115*, 2360 -–2375.
7. Daughtry, C.; Walthall, C.; Kim, M.; de Colstoun, E.; III, J. M. Estimating corn leaf chlorophyll concentration from leaf and canopy reflectance. *Remote Sens. Environ.* **2000,** *74*, 229–239.
8. Hunt, E. R.; Rock, B. N. Detection of changes in leaf water-content using near-infrared and middle-infrared reflectance. *Remote Sens. Environ.* **1989,** *30*, 43–54.
9. Dash, J.; Curran, P. J. The MERIS terrestrial chlorophyll index. *Int J Remote Sens.* **2004,** *25*, 5403–5413.
10. Tucker, C. J. Red and photographic infrared linear combinations for monitoring vegetation. *Remote Sens. Environ.* **1979,** *8*, 127–150.
11. Gamon, J.; nuelas, J. P.; Field, C. A narrow-waveband spectral index that tracks diurnal changes in photosynthetic efficiency. *Remote Sens. Environ.* **1992,** *41*, 35–44.
12. Zarco-Tejada, P. J.; Gonzalez-Dugo, V., Williams, L. E.; Suarez, L.; Berni, J. A. J.; Goldhamer, D.; Fereres, E. A PRI-based water stress index combining structural and chlorophyll effects: Assessment using diurnal narrow-band airborne imagery and the CWSI thermal index. *Remote Sens. Environ.* **2013,** *138*, 38–50.
13. Garrity, S. R.; Eitel, J. U.; Vierling, L. A. Disentangling the relationships between plant pigments and the photochemical reflectance index reveals a new approach for remote estimation of carotenoid content. *Remote Sens. Environ.* **2011,** *115*, 628–635.
14. Blackburn, G. A. Quantifying chlorophylls and carotenoids at leaf and canopy scales: An evaluation of some hyperspectral approaches. *Remote Sens. Environ.* **1998,** *66*, 27– 285.
15. Boochs, F.; Kupfer, G.; Dockter, K.; Kühbauch, W. Shape of the red-edge as vitality indicator for plants. *Int J Remote Sens.* **1990**, *11*, 1741–1753.
16. Lichtenthaler, H. K.; Lang, M.; Sowinska, M.; Heisel, F.; Miehe, J. A. Detection of vegetation stress via a new high resolution fluorescence imaging system. *J. Plant Physiol.* **1996,** *148*, 599–612.
17. Hernández-Clemente, R.; Navarro-Cerrillo, R. M.; Zarco-Tejada, P. J. Carotenoid content estimation in a heterogeneous conifer forest using narrow-band indices and PROSPECT + DART simulations. *Remote Sens. Environ.* **2012,** *127*, 298–315.
18. Elvidge, C. D.; Chen, Z. K. Comparison of broad-band and narrow-band red and near-infrared vegetation indexes. *Remote Sens. Environ.* **1995,** *54*, 38–48.
19. Filella, I.; Pe˜ nuelas, J. The red edge position and shape as indicators of plant chlorophyll content, biomass and hydric status. *Int J Remote Sens.* **1994,** *15*, 1459–1470.
20. Vogelmann, J. E.; Rock, B. N.; Moss, D. M. Red edge spectral measurements from sugar maple leaves. *Int J Remote Sens.* **1993,** *14*, 1563–1575.